Dolling and Cowley recently have succeeded in fitting the inelastic neutron scattering dispersion relationships for diamond, Si, Ge, and GaAs with a shell-model calculation.[8] They have been able to reproduce the observed Θ-versus-T relations for these solids, and by means of two adjustable parameters which reflect the volume dependence of two of the shell-model parameters, they have been able to reproduce the higher-temperature thermal-expansion behavior. The qualitative change in shape of the lowest transverse-acoustic dispersion relation with decreasing volume is confirmed, and a discrepancy with respect to the high-pressure elastic-constant measurements for this mode is reported. They do not give a value of γ_0 since the grid of points which they used was not sufficiently fine to give a reliable value. Approximate values of γ_0 can be calculated within these limitations, however, which are surprisingly close to the values which we observe (Table V).[40] No basis for a discrepancy between γ_0^{th} and γ_0^{el} exists in the theory.

Note added in proof. Dr. D. E. Schuele of the Case Institute of Technology has used the high-pressure elastic-constant data given in Refs. 36, 37, and 39, and a computer program which uses 184 equally spaced points over the unit triangle of a cubic crystal [J. Phys. Chem. Solids **25**, 801 (1964)] to calculate γ_0's for Si, Ge, and GaAs. The γ_0's calculated for the 77°K Si and Ge data (0.211 and 0.480, respectively) agree with those given in Table V. The γ_0 calculated for the room-temperature GaAs data (0.367) perhaps should be reduced by from 5 to 10% (by analogy with Ge) to obtain a true absolute zero value. The resulting estimate of 0.35 is to be compared with our thermal value of 0.58 (Table III). The authors are indebted to Dr. Schuele for carrying out these calculations.

[40] R. A. Cowley (private communication).

PHYSICAL REVIEW VOLUME 163, NUMBER 3 15 NOVEMBER 1967

Electrical Studies of Electron-Irradiated *n*-Type Si: Impurity and Irradiation-Temperature Dependence*

HERMAN J. STEIN AND FREDERICK L. VOOK
Sandia Laboratory, Albuquerque, New Mexico
(Received 3 May 1967)

Electrical-conductivity and Hall-coefficient measurements have been used to investigate the crystal growth and irradiation-temperature dependence of the introduction and annealing of defects in electron-irradiated *n*-type silicon. Irradiations of 10-Ω cm, phosphorus-doped silicon with 1.7-MeV electrons were performed at controlled temperatures between 75 and 300°K, and isochronal annealing was investigated between 80 and 700°K. Both intrinsic defects and impurity-associated defects are observed. The impurity independence of annealing between 100 and 200°K suggests the annealing of intrinsic defects. The introduction rate for these intrinsic defects is independent of the irradiation temperature between 75 and 100°K. The introduction rates for the impurity-associated defects, however, exhibit an exponential dependence on the reciprocal irradiation temperature between 75 and 100°K consistent with a model based on metastable vancacy-interstitial pairs that predicts a temperature-dependent probability for vacancy-interstitial dissociation during irradiation and subsequent trapping by crystal impurities. For irradiations above 100°K, the introduction rates of impurity-associated defects are relatively independent of the irradiation temperature. Excluding the carrier-removal annealing which is associated with the intrinsic-defect stage, 90% of the annealing in crucible-grown silicon and ~70% of the annealing in float-zone, Dash, and Lopex silicon correlate with the annealing of the divacancy and impurity-associated defects observed in EPR and optical-absorption studies on *n*-type silicon. In crucible-grown silicon, the annealing temperatures of the dominant electrically active, impurity-associated defects correlate with those for the *A* center and other oxygen-associated defects. Measurements of carrier concentration versus temperature provide additional evidence for the dominance of the *A* center which has an energy level near $E_c-0.185$ eV, where E_c is the energy of the conduction-band minimum. A level near $E_c-0.13$ eV also is observed in crucible-grown silicon for the oxygen-associated defects responsible for reverse annealing between 200 and 250°K. In float-zone silicon, the annealing temperatures of the dominant electrically active defects correlate with the *E*-center and divacancy annealing. Lopex silicon is very similar to Dash silicon, and in these materials all the annealing stages of crucible and float-zone silicon are observed.

I. INTRODUCTION

INTRINSIC structural defects such as vacancies and interstitials are produced in silicon crystals by high-energy particle irradiation. Significant thermal reordering and impurity trapping of these defects occur below room temperature so that electrically active impurity-associated defect complexes are observed following irradiation at temperatures where the intrinsic defects are mobile.[1] To understand radiation effects in silicon,

* This work supported by the U. S. Atomic Energy Commission.

[1] For a recent review of radiation-induced defects in silicon, see J. W. Corbett, in *Solid State Physics*, edited by F. Seitz and D. Turnbull (Academic Press Inc., New York, 1966), Suppl. 7, p. 59.

it is important to determine the properties and production mechanisms of the intrinsic defects as well as to identify the resultant defect-impurity complexes.

Low-temperature irradiations of silicon crystals of known composition can be used to determine the mechanisms of defect production and to separate the properties of intrinsic defects from the properties of defect-impurity complexes which are dominant at higher temperatures. For low-temperature irradiations, the pronounced irradiation temperature dependence recently investigated by optical techniques[2] in crucible-grown silicon requires that the production of electrically active defects be investigated at controlled irradiation temperatures for all growth methods. The electrical properties of specific defect-impurity complexes can be determined by correlating electrical, optical, and electron-paramagnetic-resonance (EPR) measurements on crystals of different growth methods containing specific impurities.

In the present paper, information about the nature and the formation of electrically active radiation-produced defects has been obtained from Hall-effect and electrical-conductivity measurements on n-type silicon following 1.7-MeV electron irradiation at controlled irradiation temperatures between 75 and 300°K. Hall-effect and electrical-conductivity measurements have also been used to investigate the isochronal annealing behavior of the radiation-produced defects between 80 and 700°K. Samples were selected from silicon crystals grown by quartz-crucible, vacuum-floating-zone, Dash, and Lopex techniques to examine the influence of the crystal growth method on the electrically active defect behavior.[3]

The experimental methods, apparatus, and silicon material characteristics are discussed in Sec. II. The results of the carrier-removal and carrier-mobility measurements for electron irradiation and isochronal annealing are presented in Sec. III. These results are then discussed in Sec. IV in terms of proposed mechanisms of defect production and previous optical and EPR results that help to identify the defects.

II. EXPERIMENTAL METHODS

The Hall effect and electrical conductivity were obtained by direct current-voltage techniques on square ($5\times5\times0.5$ mm) samples of ≈10 Ω cm ($n_0\approx5\times10^{14}$), phosphorus-doped n-type silicon. Electrical contacts were made by evaporating and alloying gold with 1% antimony to the top-surface corners of the samples. A magnetic field strength of 2500 G and electric fields of ≤1 V/cm were used in the measurements. The carrier concentration and carrier mobility in the silicon samples were obtained from the Hall-coefficient and electrical-conductivity measurements.

Equation (1) gives the relationship for obtaining the carrier concentration n from the Hall coefficient R:

$$n=(\mu_h/\mu_c)(1/Rq)\,, \tag{1}$$

where μ_h/μ_c is the ratio of the Hall mobility to the conductivity mobility. The magnitude and temperature dependence of μ_h/μ_c have been empirically determined from experimental Hall-coefficient data by assuming negligible compensation of the unirradiated material and setting the ratio equal to unity at 160°K in accordance with reported measurements on the μ_h/μ_c ratio.[4] The empirical equation for the ratio is

$$\mu_h/\mu_c=0.775+3.23\times10^{-3}T-3.17\times10^{-5}T^2+2.00\times10^{-7}T^3-5.42\times10^{-10}T^4+5.23\times10^{-13}T^5. \tag{2}$$

This equation gives ratios ranging between 0.91 at 75°K to 1.23 to 360°K. The carrier mobility measured in this investigation is the Hall mobility obtained from the Hall coefficient and the electrical conductivity. Initial values for the carrier-concentration and reciprocal Hall mobilities at 80°K are listed in Table I for the sample set subsequently irradiated at 80°K.

The known material variables among the crystals of different growth methods used in the present experiment are the oxygen concentration and the dislocation density. The quartz crucible-grown crystal has an oxygen concentration of 5×10^{17} atoms per cm^3 as measured by the intensity of the 9-μ optical-absorption band.[5] The oxygen concentrations in vacuum-floating-zone, Lopex, and Dash-grown crystals are below the detectability threshold by infrared-absorption measurements at room temperature ($\leq5\times10^{16}$ cm^{-3}). Dislocation densities as measured by etch pit counting are $\approx10^4$ cm^{-2} for float-zone silicon, $\approx10^3$ cm^{-2} for crucible-grown silicon, and $\approx10^2$ cm^{-2} for Dash and Lopex silicon.

Figure 1 is a diagram of the cryostat used in the experiments. The cryostat employs a trapped-gas heat exchanger (D) and an anodized aluminum jig (B) which gives mechanical support and thermal contact to four silicon samples (A). The four samples are held against the anodized aluminum jig front face (not shown)

TABLE I. Initial carrier concentrations and reciprocal-Hall mobilities measured at 80°K.

Crystal code	Growth method	Initial n_0 (10^{14} cm^{-3})	Initial $1/\mu_0$ (10^{-5} V sec/cm^2)
AP	Crucible	4.54	7.05
P	Zone	4.24	6.62
AW	Lopex	3.67	6.74
AG	Dash	3.18	7.15

[2] R. E. Whan and F. L. Vook, Phys. Rev. **153**, 814 (1967).
[3] H. J. Stein, Bull. Am. Phys. Soc. **11**, 194 (1966); IEEE Nuclear and Space Radiation Effects Conference, Palo Alto, California, 1966 (unpublished).
[4] F. J. Morin and J. P. Maita, Phys. Rev. **96**, 28 (1954).
[5] W. Kaiser and P. H. Keck, J. Appl. Phys. **28**, 882 (1957).

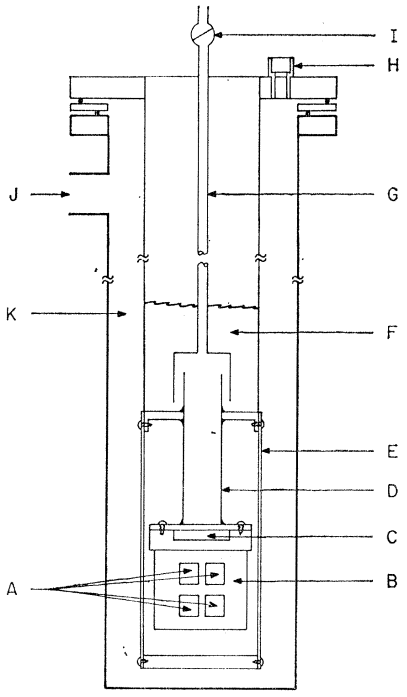

FIG. 1. Irradiation and annealing cryostat: (A) four silicon samples, (B) anodized aluminum jig, (C) heater, (D) cold finger and heat exchanger, (E) thermal shield, (F) liquid-nitrogen reservoir, (G) vent tube, (H) electrical feed-through (serum cap), (I) vent valve, (J) pumping port, and (K) vacuum space.

by spring-loaded silver pins which make electrical contact to the gold-alloyed corners on the silicon. A small dot of vacuum grease is used between the front face and the samples and between the front and back sections of the jig to improve thermal contact to the jig base. Located behind each sample is a small, tungsten filament lamp that is suitable for checking on the presence of minority carrier trapping in the silicon samples. A 20-W button heater (C) is located in the aluminum jig for temperature operation above 78°K.

The jig is secured to a thin-walled (7 mil) copper cold finger (D) which extends into the liquid-nitrogen reservoir (F). The top of the cold finger is loosely capped with a vent tube (G). When the vent tube is open, liquid nitrogen will fill the cold finger and the jig will stabilize at 78°K. To operate at 80°K, the heater is used to increase the temperature of the jig with liquid nitrogen in the cold finger. For operation above 80°K, the vent valve (I) is closed, and the heater is used to vaporize the liquid in the cold finger. After the liquid is boiled away, gas is trapped in the cold finger and forms a heat exchanger between the jig and the liquid-nitrogen reservoir. The output from a copper-constantan thermocouple soldered to the heater goes to a relay amplifier which closes a relay when the thermocouple voltage deviates more than 3 μV from a preselected control point. The relay amplifier provides on-off control of 10% of the heater voltage that is selected for control at a particular temperature. The temperature of the jig is measured by a second thermocouple positioned on the jig.

A 2-MeV Van de Graaff accelerator was used as the electron irradiation source. The electrons passed through two 5-mil aluminum windows and 20 mils of aluminum on the front face of the jig before encountering the silicon samples. The 30 mils of aluminum decrease the electron energy from 2 to 1.7 MeV.[6] The electron fluence (time-integrated flux) was obtained by charge collection from the jig and a copper shield on the back side of the jig. A $\frac{5}{8}\times\frac{5}{8}$-in. square aperture limits the scanned electron beam incident upon the aluminum jig.

The irradiation cryostat is also used for Hall-coefficient and electrical-conductivity versus temperature measurements and for isochronal annealing measurements. The cryostat can be operated at temperatures between 78 and 360°K with a temperature control of ± 0.1°K about a fixed point for the measurements before and during irradiation when sufficient time can be allowed for stabilization. To obtain a sharp rise time to the annealing point (less than one minute for the final 10 deg. to control point), the thermocouple located on the jig was used as the control thermocouple in the 20-min. annealing periods. The temperature control for this method of operation is ± 0.5°K. At the termination of the annealing period, the heater power is turned off, and the vent valve is opened to allow liquid nitrogen into the cold finger. Annealing between 360 and 700°K was performed by removing the samples from the cryostat and placing them in a dry nitrogen atmosphere tube furnace with a temperature control of ± 3°K.

III. EXPERIMENTAL RESULTS

A. Carrier-Removal Rate

Electron irradiation at 80°K decreases the electrical conductivity of n-type silicon. This effect is illustrated in Fig. 2 for phosphorus-doped silicon grown by quartz-crucible, float-zone, Lopex, and Dash techniques. There was no evidence of minority carrier trapping in any of the materials. The data indicate that the decrease in conductivity at 80°K is linearly proportional to the electron fluence (time-integrated flux) for all the crystal growth methods, but the magnitude of the decrease is crystal-growth-dependent. The smallest magnitude of the conductivity decrease with electron fluence is exhibited by the oxygen-containing crucible-grown silicon.

Since the conductivity includes both the carrier concentration and the carrier mobility, an independent determination of the carrier concentration by Hall-coefficient measurements is required to separate the effect of irradiation on the two parameters. It is common practice to describe the irradiation-produced

[6] L. B. Spencer, Natl. Bur. Std. (U. S.) Monograph 1 (1959).

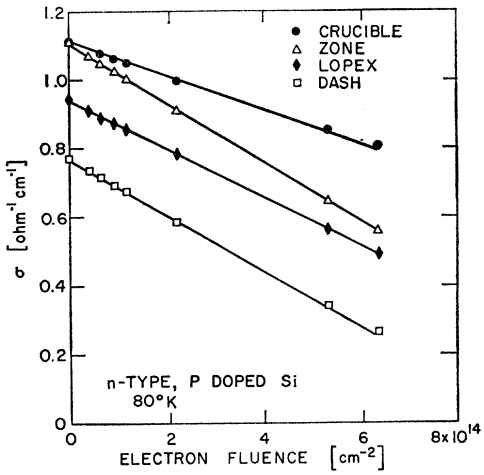

FIG. 2. Electrical conductivity versus 1.7-MeV electron fluence at 80°K for phosphorus-doped quartz-crucible, vacuum-floating-zone, Dash, and Lopex silicon.

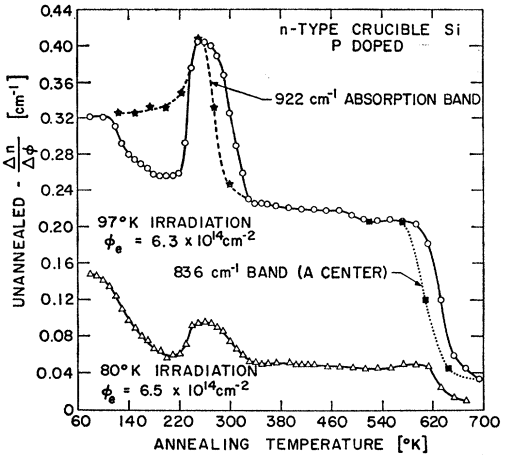

FIG. 3. Unannealed carrier-removal rate versus annealing temperature for crucible-grown silicon after irradiation at 80 and 97°K. Measurements at 80°K. A center annealing reported by Corbett *et al.* (see Ref. 9) and 922-cm^{-1} absorption-band annealing reported by Whan and Vook (see Ref. 2) included for data comparison.

decrease in carrier concentration as a carrier-removal rate ($-\Delta n/\Delta\Phi$). For the present experiments, the carrier-removal rate is the difference between the carrier concentration measured before and after irradiation divided by the total irradiation fluence. The isochronal-annealing data are presented as the unannealed carrier-removal rate which is the difference between the carrier concentration before irradiation and after 20 min at the annealing temperature, divided by the total irradiation fluence. All measurements were made at 80°K and plotted at the annealing temperature.

1. *Crucible-Grown Silicon*

The unannealed carrier-removal rate for crucible-grown, n-type silicon is shown in Fig. 3 for annealing temperatures between 80 and 700°K. The results for a 97°K-irradiation and for an 80°K-irradiation are shown. It is apparent that the unannealed carrier-removal rate is dependent upon the irradiation temperature throughout the annealing range. The magnitude of the first annealing stage between 100 and 200°K is approximately equal for the two irradiation temperatures, in contrast with a marked irradiation temperature dependence for the other annealing stages. The 97 to 80°K carrier-removal-rate ratio increases from 2.25 at 80°K to 4.4 after annealing to 200°K, then remains essentially constant between 200 and 540°K before decreasing again.

A striking feature of the annealing data for crucible-grown silicon is the reverse annealing peak at 250°K. The carrier-removal rate increases 60% between 200 and 250°K and then recovers between 250 and 350°K. This reverse annealing peak is apparently associated with the formation of oxygen containing defects since it is not observed in low-oxygen-content vacuum-floating-zone silicon (see Fig. 5). The annealing of the carrier removal between 200 and 350°K, which includes the reverse annealing peak, closely parallels that for the optically-active 922-cm^{-1} band observed in irradiated crucible-grown silicon.[2,7] Despite this apparent correlation, the reverse annealing of the carrier removal is not believed to be directly related to the 922-cm^{-1} optical absorption band[8] because the optically measured ratio of the 922-cm^{-1} band to the A-center band is considerably smaller in the crucible-grown crystal used in this investigation than observed in the optical studies by Whan,[7] and Whan and Vook.[2] The annealing of the 836-cm^{-1} optical absorption band, which Corbett *et al.*[9] have associated with the oxygen-vacancy defect in irradiated silicon, is also shown in Fig. 3 for comparison with the carrier-removal-rate data.

The carrier concentration is plotted in Fig. 4 versus reciprocal temperature for a 2.5-Ω cm sample of crucible-grown silicon. Results are given before irradiation with 5.3×10^{15} electrons per cm^2 at 88°K, as well as after irradiation and thermal annealing to 200, 250, and 350°K. These annealing temperatures are just below, on, and just above the reverse annealing peak at 250°K.

---

[7] R. E. Whan, J. Appl. Phys. **37**, 3378 (1966).

[8] H. J. Stein and F. L. Vook, Bull. Am. Phys. Soc. **12**, 346 (1967). Recent optical measurements have shown that the 922-cm^{-1} production rate varies by a factor of 10 among crucible-grown crystals, whereas, the A-center production rate varies by only a factor of 1.3 among the same crystals. Results from these optical measurements also suggest that the 922-cm^{-1} band defect contains both carbon and oxygen. The fact that the 922-cm^{-1} production rate is independent of the A-center production rate is evidence that this defect contains an interstitial silicon atom rather than a vacancy and represents one kind of defect formed by impurity trapping of silicon interstitials in the temperature range between 200 and 250°K. Based on comparisons of defect annealing in electron- and neutron-irradiated silicon, Whan (Ref. 7) has previously suggested that the 922-cm^{-1} band involves oxygen and an interstitial silicon atom.

[9] J. W. Corbett, G. D. Watkins, R. M. Chrenko, and R. S. McDonald, Phys. Rev. **121**, 1015 (1961).

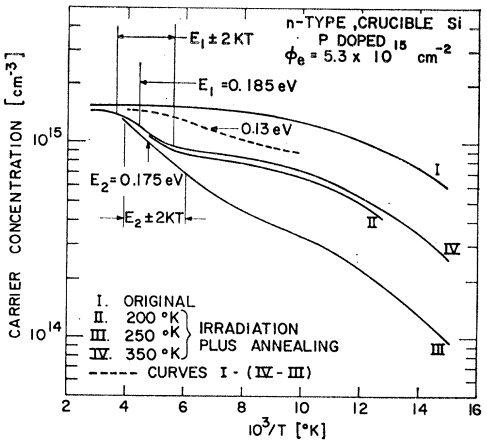

FIG. 4. Carrier concentration versus reciprocal temperature for crucible silicon before irradiation and after irradiation at 80°K plus annealing to 200, 250, and 350°K.

There is clear evidence for the existence of defect energy levels after irradiation and annealing.

For a single defect level with an equal number of ways of being occupied and unoccupied, the probability f that the center will be occupied with an electron is

$$f=\{1+\exp[(E_d-E_F)/kT]\}^{-1}. \quad (3)$$

The Fermi level (E_F) coincides with the energy of the defect level (E_d) when f is $\frac{1}{2}$. A single energy level at E_d should vary between 88% and 12% filled as the Fermi level moves from $2kT$ above the defect level to $2kT$ below the level. The reciprocal temperature width corresponding to $E_d \pm 2kT$ is included in Fig. 4 for E_d equal to 0.185 and 0.175 eV. For anneals to 200°K and to 350°K (below and above the reverse annealing peak), the temperature dependence of the carrier concentration is consistent with the A-center energy level at 0.185 eV below the conduction band. However, the carrier concentration versus temperature obtained after annealing to 250°K (peak of reverse annealing) gives a wider temperature range than expected for a single level which might be estimated to be at 0.175 eV below the conduction band.

Assuming that the concentration of the 0.185-eV defect level is constant for annealing between 250 and 350°K, an estimate can be made of the position of the additional energy level associated with the reverse annealing. The result of subtracting the effects of the 0.185-eV level from the carrier-concentration–versus–temperature measurements in the reverse annealing peak is shown as a dashed line in Fig. 4. This line represents the expected carrier concentration versus temperature if only the defect responsible for the reverse annealing were present and is obtained by subtracting the difference between curves IV and III from curve I. The carrier concentration versus temperature indicated by the dashed line is consistent with an energy level $\approx$0.13 eV below the conduction band. This result suggests that this energy level is associated with the defects responsible for the reverse annealing.[10]

Measurements of the carrier concentration as a function of temperature also have been made after annealing to 473 and 573°K. The results are essentially the same as those obtained after annealing to 350°K and indicate that the A center dominates the carrier removal until the major recovery stage is reached near 600°K.

2. *Float-Zone, Dash, and Lopex Silicon*

Unannealed carrier-removal rates as a function of annealing temperature are presented in Fig. 5 for 80 and 97°K irradiations of float-zone silicon. The results show that the carrier-removal rate is irradiation temperature-dependent in the low-oxygen-content, float-zone material was well as in the high-oxygen-content, crucible-grown silicon.

Float-zone silicon exhibits a carrier-removal recovery between 100 and 200°K following irradiation at 80°K that is equal in magnitude to that observed in crucible-grown silicon. This recovery stage for the 97°K irradiation is interrupted by reverse annealing which peaks at 160°K (Fig. 5). Two large recovery stages are observed in float-zone silicon near 420 and 560°K which were not observed in crucible-grown silicon. The stage near 420°K correlates in temperature with the annealing of the vacancy-phosphorus complex (E center),[11,12]

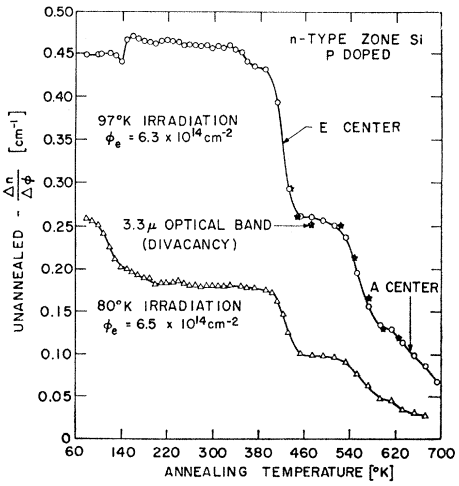

FIG. 5. Unannealed carrier-removal rate versus annealing temperature for float-zone silicon after irradiation at 80 and 97°K. Measurements at 80°K. Divacancy annealing reported by Cheng *et al.* (see Ref. 14) included for data comparison.

[10] The $E_c-0.185$-eV level is deeper than the $E_c-0.17$-eV level frequently quoted for the A center. (E_c is the energy of the conduction-band minimum.) However, $E_c-0.185$ eV is in good agreement with the temperature-dependent value of $E_c-(0.16+1.1\times10^{-4}T)$ eV given by Wertheim (Ref. 23), where $T\simeq220$°K in the present experiment.

[11] H. Saito, M. Hirata, and T. Horiuchi, J. Phys. Soc. Japan 18, Suppl. 3, 246 (1963).

[12] G. D. Watkins and J. W. Corbett, Phys. Rev. 134, A1359 (1964).

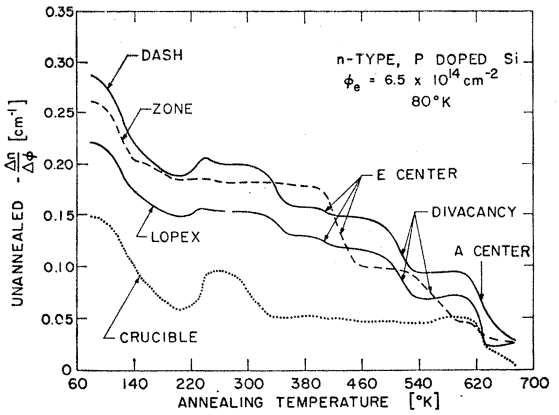

FIG. 6. Unannealed carrier-removal rates for quartz-crucible, float-zone, Dash, and Lopex silicon after irradiation at 80°K. Measurements at 80°K.

and the stage near 560°K correlates in temperature with the annealing of the divacancy.[13,14] The annealing of the 3.3-μ absorption band which Cheng *et al.*[14] have associated with the divacancy is plotted in Fig. 5 and compares closely to the carrier-removal-rate annealing data between 440 and 600°K. Additional carrier-removal recovery is observed between 600 and 700°K which is the temperature range for A-center annealing in crucible-grown silicon. The pronounced reverse annealing peak observed at 250°K in crucible-grown silicon is not observed in float-zone silicon.

The unannealed carrier-removal rates for float-zone, crucible-grown, Dash, and Lopex silicon following an 80°K irradiation are compared in Fig. 6. The dashed and dotted lines are the results from float-zone and crucible-grown silicon which were shown in Figs. 3 and 5. The solid lines are the results from Lopex- and Dash-grown silicon which are the low-dislocation-content, low-oxygen-content materials. The 100 to 200°K annealing stage is observed in all the materials, independent of the crystal-growth method. For temperatures above 200°K, the annealing behavior for Lopex- and Dash-grown silicon is intermediate between that for the float-zone and that for the crucible-grown silicon; however, the magnitude of the carrier-removal rate for the Dash- and Lopex-silicon is more nearly equal to that of the float-zone silicon than to that of the crucible-grown silicon.

B. Irradiation-Temperature Dependence

Figure 7 shows the irradiation-temperature dependence of the carrier-removal rate for float-zone and crucible-grown silicon. For irradiation temperatures below 200°K, the data were obtained after the samples were annealed to 200°K to eliminate the defects annealing in the 100 to 200° K stage. A different sample was used for each irradiation temperature with all the samples for one crystal-growth method prepared from the same crystal. The results show an exponential dependence of the carrier-removal rate upon the reciprocal irradiation temperature for irradiation temperatures below 100°K. Above 100°K, a tendency toward saturation is observed. Above 200°K, defect annealing is observed in the irradiation-temperature dependence of the carrier-removal rate, particularly, the 250°K reverse annealing peak in crucible-grown silicon.

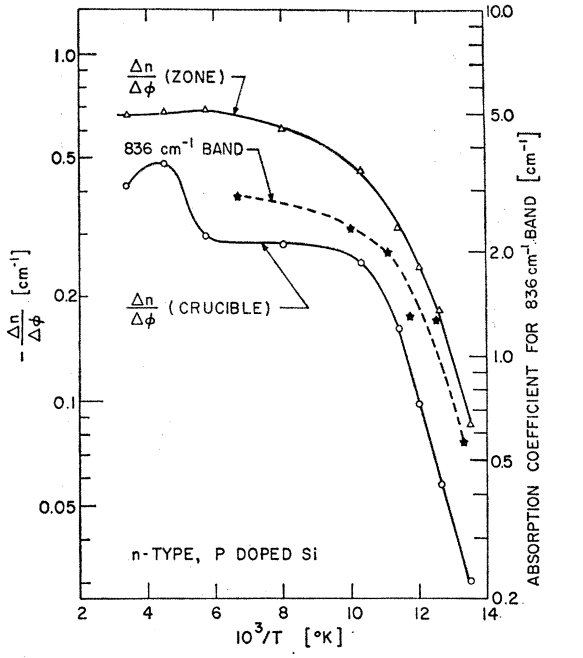

FIG. 7. Carrier-removal rates versus reciprocal irradiation temperature for float-zone and quartz-crucible silicon. Measurements at 80°K after annealing to 200°K. Intensity of 836-cm^{-1} (A center) band from results of Whan and Vook (see Ref. 2) after 10^{18} electrons/cm^2 and annealing to 175°K.

Although the irradiation-temperature dependence of the carrier-removal rate is similar in float-zone and crucible-grown silicon, the removal rates are approximately a factor of two larger in float-zone silicon than in crucible-grown silicon. The irradiation-temperature dependence for the A-center optical-absorption band[2] after annealing to 175°K is also shown in Fig. 7 for comparison with the carrier-removal data.

A similar experiment to that yielding the results of Fig. 7 was performed by reirradiating samples for all irradiation temperatures in the following sequence: 125, 74, 79, 85, and 95°K. To minimize the residual damage, the samples were annealed for 1 h at 400°C before each reirradiation. The results for all crystal-growth methods are shown in Fig. 8. The experiment was performed in this manner because it was impossible to obtain reproducible carrier-removal results on different samples of Dash and Lopex silicon. A variation in the oxygen

[13] G. D. Watkins and J. W. Corbett, Phys. Rev. **138**, A543 (1965).
[14] L. J. Cheng, J. C. Corelli, J. W. Corbett, and G. D. Watkins, Phys. Rev. **152**, 761 (1966).

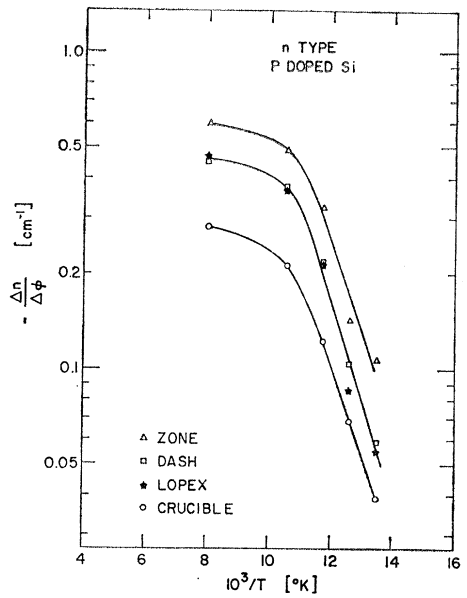

FIG. 8. Carrier-removal rates versus reciprocal irradiation temperature for float-zone, quartz-crucible, Dash, and Lopex silicon. Measurements at 80°K after annealing to 200°K. Same samples used throughout experiment by annealing at 400°C after each irradiation with 6.7×10^{14} electrons/cm^2.

concentration of the Dash and Lopex samples is believed to be responsible for the lack of reproducibility in the measured carrier-removal rate in these materials. Although oxygen cannot be detected in Lopex- and Dash-grown silicon by the 9-μ absorption at room temperature, it is detectable when the measurement temperature is lowered to 80°K. Optical absorption at 9 μ is not detectable at 80°K, however, in the float-zone silicon.

The reirradiation of previously irradiated and annealed samples gives a slightly smaller slope of $k[\ln(\Delta n/\Delta\Phi)]$ versus $1/T$ for crucible-grown material (0.055 eV) than do measurements on samples without an irradiation history (0.071 eV). This difference, however, cannot be attributed to the irradiation history of the samples since infrared-absorption measurements of A-center production in crucible-grown crystals without an irradiation history gave a slope of 0.05±0.005 eV.[2] The slopes for the other materials in this study are also 0.06±0.01 eV. These variations in observed slopes probably reflect the fact that a 1°K error in irradiation temperature near 80°K yields approximately 15% error in the carrier-removal rate. Therefore, it is concluded that, to within the experimental uncertainties, the same basic irradiation-temperature dependence is observed in silicon of all growth methods.

C. Carrier-Mobility Changes

The experimental mobility changes have been plotted as the increase in the reciprocal Hall mobility because, to the first approximation, the reciprocal impurity mobility (μ_I) is proportional to the total concentration (N_I) of ionized donors (N_D) and acceptors (N_A),[15] according to the equation

$$1/\mu_I=\frac{\eta N_I\{\ln b-1\}}{T^{3/2}}, \tag{4}$$

$$\eta=\frac{\pi^{3/2}e(q)^2m^{1/2}}{2^{7/2}k^{3/2}\epsilon^2}, \tag{5}$$

$$b=\frac{24\pi m\epsilon(kT)^2}{n'e^2h^2}, \tag{6}$$

$$n'=n+(n+N_A)[1-(n+N_A)/N_D], \tag{7}$$

where m is the electron effective mass, e is the electron charge, ϵ is the dielectric constant, and q is the charge on the scattering center. It is further assumed that the defect-produced impurity mobility (μ_{Id}) is related to the experimental measurements of the Hall mobility before irradiation (μ_{bi}) and after irradiation (μ_{ai}) by the equation

$$\frac{1}{\mu_{Id}}=\frac{1}{\mu_{ai}}-\frac{1}{\mu_{bi}}. \tag{8}$$

This expression is valid only if all scattering mechanisms are independent and exhibit the same dependence upon electron energy.[16] It is apparent that more assumptions are made regarding the relationship between the mobility change and the change in impurity-scattering-center concentration than are made when relating the carrier-removal rate to the introduction rate of the impurity defect. However, the mobility results provide

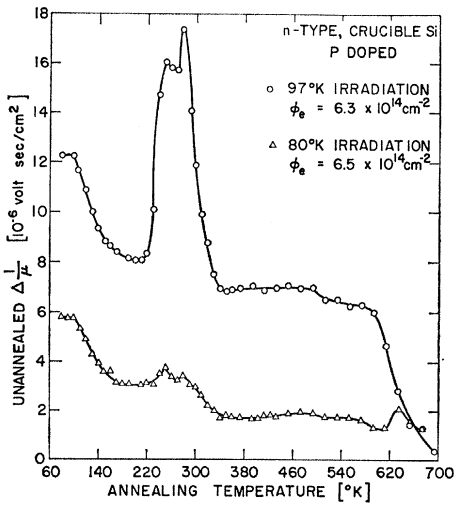

FIG. 9. Unannealed change in reciprocal mobility for quartz-crucible-grown silicon following irradiation at 80 and 97°K. Measurements at 80°K.

[15] D. Long and J. Myers, Phys. Rev. **115**, 1107 (1959).
[16] N. B. Hannay, *Semiconductors* (Reinhold Publishing Corporation, New York, 1959), p. 346.

valuable information on the relative charge of defects involved in thermal reordering since the reciprocal mobility depends on the second power of the charge on the scattering center.

1. Crucible-Grown Silicon

The unannealed increase in reciprocal mobility as a function of annealing temperature is shown in Fig. 9 for crucible-grown silicon irradiated at 80 and 97°K. The irradiation-temperature dependence and the annealing behavior of the reciprocal mobility are similar to those obtained from the measurements of the carrier-removal rate but show some additional structure. The reverse annealing peak observed at 250°K in the carrier removal appears to be a double peak in the mobility annealing, where the first of the two peaks correlates with annealing of the 922-cm^{-1} optical-absorption band shown in Fig. 3. The major recovery stage near 600°K is shifted slightly toward a lower temperature compared with the carrier-removal annealing, and a reverse annealing peak is observed at 640°K after the 80°K irradiation.

2. Float-Zone, Dash, and Lopex Silicon

The mobility-annealing behavior for the float-zone silicon between 80 and 700°K is shown in Fig. 10. The increase in reciprocal mobility for irradiation at 97°K is essentially equal to the increase for irradiation at 80°K immediately after irradiation; however, the 97 to 80°K damage ratio approaches that for the carrier-removal rate after annealing to 250°K. The mobility-annealing behavior above 250°K is somewhat different from that for the carrier-removal rate in this material. In particular, the annealing stage observed near 420°K in the carrier-removal rate is not observed as a recovery in the mobility annealing but rather as a small reverse annealing.

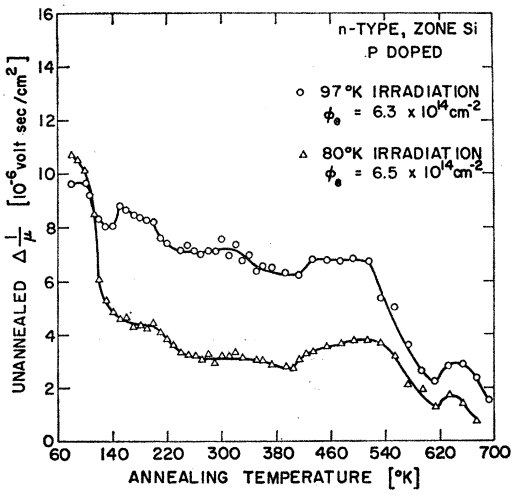

FIG. 10. Unannealed change in reciprocal mobility for float-zone silicon following irradiation at 80 and 97°K. Measurements at 80°K.

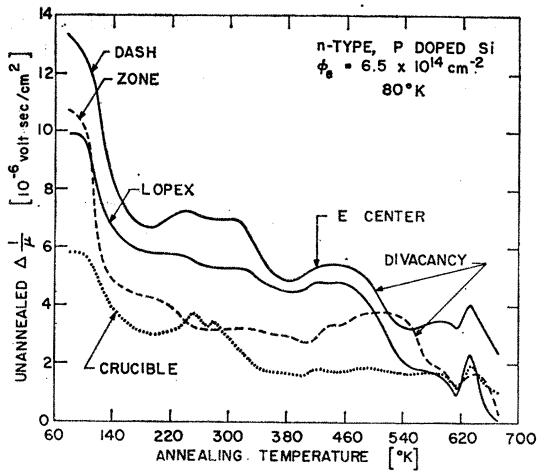

FIG. 11. Unannealed change in reciprocal mobility for float-zone, quartz-crucible, Dash, and Lopex silicon following irradiation at 80°K. Measurements at 80°K.

The unannealed changes in the reciprocal carrier mobilities for float-zone, crucible-grown, Dash, and Lopex silicon following irradiation at 80°K are compared in Fig. 11. The crucible-grown and float-zone silicon results are the same as those presented in Figs. 9 and 10. The magnitude of the mobility recovery between 100 and 200°K is misleadingly small for crucible-grown silicon due to simultaneous reverse annealing. This effect is more pronounced in the mobility recovery than in the carrier-removal recovery. The mobility-annealing results for Dash and Lopex silicon are similar, as shown by the solid lines in Fig. 11. In general, the stages observed in the carrier-removal annealing are also observed in the mobility annealing, and stages which correlate in temperature with the E-center and divacancy defects are labeled in Fig. 11.

IV. DISCUSSION

The formation, annealing, and trapping of intrinsic defects are discussed first. These defects anneal primarily at lower temperatures than do the defect-impurity complexes which are discussed in the second subsection. Although the divacancy is an intrinsic defect by this definition, it is discussed in the second subsection since it anneals at a higher temperature than some vacancy-impurity complexes. Furthermore, the concentration of divacancies, as measured by the magnitude of the corresponding annealing stage, appears to be dependent upon the lower-temperature annealing of vacancy-impurity complexes.

A. Intrinsic Defect Formation, Annealing, and Trapping

The results indicate that two predominant kinds of defects are formed in n-type silicon under 1.7-MeV elec-

tron irradiation. One kind of defect exhibits an irradiation-temperature dependence consistent with the production of metastable interstitial-vacancy close-pairs and subsequent impurity trapping of the liberated vacancies and interstitials.[2] The details of the metastable close-pair model and its application to the experimental results will be discussed later. The second kind of defect is introduced at a rate that is irradiation-temperature-independent, and these defects will be referred to as ITI defects.

The ITI defects are produced at a rate independent of the irradiation temperature between 75 and 100°K, and they anneal between 100 and 200°K as shown in Fig. 3. The production rate of these defects is also independent of the crystal-growth method as shown by the data for Dash, float-zone, Lopex, and crucible-grown silicon in Fig. 6. The irradiation-temperature independence and apparent impurity independence of the introduction rate for the ITI defects suggest that they are intrinsic defects.[17]

Carrier-concentration–versus–temperature measurements give no indication of energy levels between 0.05 and 0.09 eV below the conduction band for the ITI defects, implying that their associated energy levels are ≥ 0.1 eV below the conduction band. The irradiation-produced mobility changes indicate that these defects are efficient charge scattering centers. The ratio of the mobility recovery to the carrier-removal recovery is approximately a factor of 2 larger for the ITI defects than for the single charged A center. This suggests that the ITI defects are doubly charged.

Defect annealing which may be attributed to the ITI defects has also been observed for 45-MeV electron irradiation[18] and reactor-neutron irradiation[19] but is not observed for 300-keV electron irradiation.[20] The carrier-removal rate attributable to these defects is approximately a factor of 5 larger for the 45-MeV electron irradiation and approximately a factor of 8 larger for reactor-neutron irradiation than for the 1.7-MeV electron irradiation. The increase in the production rate of the ITI defects with an increase in bombardment energy is in contrast with the elimination of the irradiation-temperature dependence of the impurity-associated defect production as the electron bombardment energy is increased above threshold.[18] These results imply that the ITI defects are produced by a process distinct from that responsible for the impurity-associated irradiation-temperature-dependent defect production. Since the irradiation-temperature dependence for impurity-associated defect production is most pronounced for the low-energy irradiation, this effect must be produced by near-threshold displacements and is consistent with the metastable pair model. The bombardment energy dependence of the ITI defect production suggests that these defects are produced when the struck atom receives an energy in excess of that required for the production of a metastable close-pair model. The broad annealing temperature range for the ITI defects also suggest more complicated annealing kinetics than simple close-pair recombination. Further work is necessary to determine the more detailed properties of the ITI defects and their production mechanism.

Infrared-absorption studies of the irradiation-temperature dependence of the production rate for oxygen-associated defect-complexes in silicon have been interpreted to give the temperature dependence of free vacancy and interstitial formation. Whan and Vook[2] have shown that the vacancy-production rate obtained in the infrared-absorption study is consistent with a model which predicts a temperature-dependent probability for close-spaced vacancies and interstitials to separate and form complexes with oxygen in silicon. On the basis of the model, the fraction (F) of the vacancies which are liberated from their corresponding interstitials is given by

$$F=\frac{1}{1+\gamma \exp[(E_b-E_a)/kT]}, \tag{9}$$

where E_a and E_b are the energy barriers for vacancy annihilation and vacancy liberation, respectively, and γ is the ratio of the statistical weights for the jump which annihilates the vacancy-interstitial pair to that which liberates the vacancy and its corresponding interstitial. When E_b is greater than E_a, and T is small, then $\exp[(E_b-E_a)/kT]$ is $\gg 1$, and F is proportional to $\exp[-(E_b-E_a)/kT]$. Thus, the slope of $k(\ln F)$ plotted against $1/T$ gives the difference in barrier heights (E_b-E_a).

Carrier-concentration measurements as a function of temperature for crucible-grown silicon suggest that the A center dominates the carrier-removal rate after annealing the ITI defects. Applying the metastable-pair model to the carrier-removal rate data after annealing to 200°K for crucible-grown silicon (Figs. 7 and 8) gives values for E_b-E_a between 0.055 eV and 0.071 eV. These values are consistent with the barrier height difference of 0.05 ± 0.005 eV obtained from A-center optical-absorption measurements made immediately after irradiation without warmup,[2] and with the irradiation-temperature dependence of the A-center optical absorption after annealing to 175°K as shown in Fig. 7. The difference in barrier height values obtained in this experiment are also consistent with the 0.067- to 0.072-eV values obtained from electrical measurements on n-type crucible-grown silicon irradiated near threshold (225- to 300-keV electrons).[20]

Since the irradiation-temperature dependence of the carrier-removal rate for float-zone, Lopex, and Dash-

[17] The 100- to 200-°K annealing stage correlates in temperature with the major recovery stage in the thermal conductivity annealing of electron-irradiated high-purity silicon [F. L. Vook, Phys. Rev. **140**, A2014 (1965)].

[18] L. J. Cheng and J. C. Corelli, Phys. Rev. **140**, A2130 (1965).

[19] H. J. Stein, following paper, Phys. Rev. **163**, 801 (1967).

[20] R. L. Novak, Ph.D. thesis, University of Pennsylvania, 1964 (unpublished).

grown silicon is essentially the same as that for the A-center-dominated crucible-grown silicon, vacancy-associated defects other than the A center can also be used as a monitor of the irradiation-temperature dependence of the liberated vacancies. This gives evidence, in addition to the bombarding-electron-energy dependence, that the irradiation-temperature dependence arises from an intrinsic production process.[21–24]

The tendency toward saturation of the carrier-removal rate for irradiation temperatures above 100°K occurs at a lower temperature than would be predicted by the model with a barrier height difference of 0.05 eV. The cause of this "bendover" or tendency toward saturation above 100°K is not completely understood. The present results show that the "bendover" occurs for fluences as low as 6.5×10^{14} e/cm^2. For fluences of this magnitude, the carrier-removal rates at a given temperature are independent of the fluence, and the "bendover" therefore is not caused by a nonlinear carrier removal. [*Note added in proof.* A model which can explain the present data, including the bendover temperature, incorporates a charge-state-dependent separation probability for the metastable pair. This model has been proposed to explain a shift in "bendover" temperature with resistivity. See F. L Vook and H. J. Stein, in Proceedings of the Santa Fe Conference on Radiation Effects in Semiconductors, October 1967, edited by F. L. Vook (to be published); B. L. Gregory and C. E. Barnes, *ibid.*]

B. Divacancy and Defect-Impurity Complex Annealing

Intrinsic-defect annealing between 100 and 200°K was discussed in the previous subsection. In this subsection, correlations of the carrier-removal rate and mobility annealing between 200 and 700°K are made with annealing data for specific defects identified in EPR[1] and optical-absorption[2] studies. These correlations of the annealing characteristics with specific-defect annealing indicate that crystal impurities compete and trap the free vacancies and interstitials formed by the irradiation.

The predominant annealing characteristics of the high-oxygen-content crucible-grown silicon correlate in temperature with the annealing of the A center and a defect which anneals in parallel with the 922-cm^{-1} optical-absorption band. The predominant annealing characteristics of the low-oxygen-content float-zone silicon correlate in temperature with the annealing of the E center and the divacancy. The annealing characteristics of the Lopex- and Dash-grown silicon indicate the presence of all the defects observed in float-zone and crucible-grown silicon, which is consistent with the larger oxygen concentration observed in Lopex- and Dash-grown silicon than in float-zone silicon. None of the annealing characteristics can be correlated with the dislocation density for the materials of this investigation.

The carrier-removal and carrier-mobility annealing results for crucible-grown silicon are similar, although some differences exist. The mobility annealing shows some structure in addition to that observed in carrier removal, and indicates that the reverse annealing peak at 250°K is actually a double peak. Evidence for multiple defect annealing between 200 and 350°K was found in optical studies on irradiated silicon by Whan,[7] and Whan and Vook.[2] Optically-active bands at 932 and 936 cm^{-1}, in addition to the 922-cm^{-1} band were observed to anneal between 250 and 325°K. If one defect which anneals in this temperature range is doubly charged, it would be more apparent in mobility measurements than in the carrier-concentration measurements, and thus produce the resolved structure in the mobility results between 200 and 350°K.

The reverse-mobility annealing near 640°K in the temperature range where the A center vanishes is more complex than can be explained by the simple loss of the A center. The complex behavior in the temperature range where the A center vanishes is consistent with the reported growth of the 887-cm^{-1} optical-absorption band in electron-irradiated silicon when the A center anneals.[25]

The annealing loss of the E-center defect near 420°K is accompanied by a recovery in the carrier-removal rate and a reverse annealing in the mobility. This behavior is expected if some divacancies or A centers are formed from the vacancies liberated during the E-center annealing. If the vacancies annealed without further defect formation at this point, the mobility change should be quite small, contrary to the observed results, since the annealing would represent a transition from a negative E center to a positive phosphorus center.

The major mobility-recovery stage in float-zone silicon correlates in temperature with the annealing of the divacancy. Therefore, it is suggested that the irradiation-produced decrease in mobility in this material is dominated by the formation of divacancies.

The annealing behavior of Lopex- and Dash-grown silicon are quite similar and show annealing stages which

[21] There is additional information in the literature on the irradiation-temperature dependence of electrically active defect production in n-type silicon that is consistent with the results under discussion. Watkins *et al.* (Ref. 22) have reported that the A-center production by 1.5-MeV electrons is a factor of 40 larger at room temperature than at 20°K followed by annealing to room temperature. Wertheim (Ref. 23) reported that the A-center production by 0.7-MeV electrons is a factor of 40 larger at room temperature than at 78°K and annealing to room temperature. Stein (Ref. 24) reported that minority carrier-lifetime degradation in n-type, float-zone silicon by Co^{60} γ rays is a factor of 20 larger at room temperature than at 76°K and annealing to room temperature.

[22] G. D. Watkins, J. Corbett, and R. Walker, J. Appl. Phys. **30**, 1198 (1959).

[23] G. K. Wertheim, Phys. Rev. **115**, 568 (1959); **110**, 1272 (1958).

[24] H. J. Stein, Appl. Phys. Letters **2**, 235 (1963); J. Appl. Phys. **37**, 3382 (1966).

[25] J. W. Corbett, G. D. Watkins, and R. S. McDonald, Phys. Rev. **135**, A1381 (1964).

correlate with those for the divacancy, E center, and A center. The divacancy annealing in Lopex- and Dash-grown silicon is shifted to lower temperatures than observed in the float-zone silicon. This is consistent with the higher oxygen content in Dash and Lopex silicon than in float-zone silicon. Watkins and Corbett[13] have also reported that the divacancy annealing is shifted to lower temperatures with an increase in the oxygen content.[26] Some reverse annealing is observed between 200 and 250°K, and the E-center annealing stage is small in Dash and Lopex silicon, which is also consistent with the higher-oxygen content in these materials than in float-zone silicon.

C. Carrier-Removal Values and Defect Inventory

The formation of the E center in float-zone silicon rather than the A center which forms in the high-oxygen-content crucible-grown silicon is primarily responsible for the larger carrier-removal rate observed in float-zone silicon than in crucible-grown silicon after annealing to 200°K. Remembering that charge neutrality must be maintained in a sample, it can be understood that when a vacancy is trapped by interstitial oxygen in n-type silicon at low temperature, the neutral oxygen defect is transformed to a neagtive A-center complex, thus removing one conduction electron. Trapping of the vacancy by the substitutional-phosphorus-defect changes the positive phosphorus to a negative E-center complex and requires the removal or two conduction electrons. Therefore, the formation of an E center by the trapping of a vacancy removes twice as many carriers as the formation of an A center.

Correlations of the annealing stages observed in the carrier removal and the mobility decrease with specific defects permits a defect inventory based upon the carrier-removal rate. For the 97°K irradiations, the carrier-removal rate inventory per incident electron for crucible-grown silicon is the following: 0.075 cm^{-1} ITI defects (first stage annealing), 0.177-cm^{-1} A centers, 0.184-cm^{-1} defects with the 0.13-eV activation energy, and 0.014 divacancies. For float-zone silicon, the inventory is: 0.075 cm^{-1} ITI defects, 0.204-cm^{-1} E centers, 0.125 cm^{-1} divacancies, and 0.125-cm^{-1} A centers and others.[27]

Since the irradiation-temperature dependence data shown in Fig. 8 of this report indicate that the defect production is essentially independent of the irradiation temperature between 97 and 300°K, the A center and divacancy production at 97°K in the present study can be compared to the 0.14-cm^{-1} and 0.009-cm^{-1} production rates for the A center and divacancy in EPR studies[28] for 1.7-MeV electron-irradiated crucible-grown silicon at 300°K. The agreement between the defect production rates observed in EPR studies and in the present study are within the combined production-rate uncertainties for the EPR and the electrical measurements.

The production-rate results indicate that the major defects resolved in EPR studies on irradiated n-type silicon are also the dominant electrically-active defects. Aside from the intrinsic ITI defects which anneal between 100 and 200°K, 90% of the carrier removal in crucible-grown silicon and ~70% of the carrier removal in float-zone, Dash, and Lopex silicon correlate with the annealing behavior of defects observed in EPR and optical studies on n-type silicon.

ACKNOWLEDGMENT

The authors wish to acknowledge the assistance of R. H. Baxter in all phases of the measurements.

[26] The assignment of the 500- to 600-°K annealing stage to the divacancy is based upon the correlation with the annealing of the 1.8- and 3.3-μ optical-absorption bands which Cheng *et al.* (Ref. 14) have associated with the divacancy. The shift to lower temperatures with higher oxygen content is also consistent with the annealing of the divacancy (Ref. 13). The ratio of the mobility recovery to the carrier-removal recovery for a doubly charged divacancy should be twice that for a singly charged center such as the A center. The results, however, show only a 20% larger ratio for the 500- to 600-°K annealing stage in float-zone silicon than for the A-center recovery stage in crucible-grown silicon. But A-center annealing also has been reported to occur between 500 and 600°K in float-zone silicon (Ref. 25). It is therefore possible that there is simultaneous A center and divacancy annealing in float-zone, Lopex-, and Dash-grown silicon. Additional investigations are required on the relationship of divacancy and A center annealing in this temperature range.

[27] According to the models for the E center and the divacancy (Ref. 1) and the present observations on the doubly charged nature of the ITI defects, the actual defect-production rate for these defects would be one-half the observed carrier-removal rates. The carrier-removal rate attributed to E-center production as determined from the magnitude of the associated-annealing stage is smaller than the actual production rate since additional defects are formed during E center annealing. The reverse annealing of carrier mobility during E center annealing provides evidence for such additional defect formation (see Fig. 10). One of the defects formed during E center annealing is probably the divacancy since the observed magnitude for the divacancy annealing stage is irradiation-temperature-dependent (see Fig. 5) and a factor of 9 larger in float-zone silicon than in crucible-grown silicon.

[28] J. W. Corbett and G. D. Watkins, Phys. Rev. **138**, A555 (1965).